Electronic Supplementary Information

Chemical functionalization of N-doped carbon nanotubes: a powerful approach to cast light on the electrochemical role of specific N-functionalities in the Oxygen Reduction Reaction

Giulia Tuci,[a] Claudio Zafferoni,[b] Andrea Rossin,[a] Lapo Luconi,[a] Antonella Milella,[c] Matteo Ceppatelli,[a,d] Massimo Innocenti,[b] Yuefeng Liu,[e,f] Cuong Pham-Huu,[e] and Giuliano Giambastiani[a,g,]*

[a] *Institute of Chemistry of OrganoMetallic Compounds, ICCOM-CNR and INSTM Consortium, 50019 Sesto F.no, (Florence), Italy. Fax: +39 055 5225203.*

[b] *Department of Chemistry, University of Florence, 50019 Sesto F.no, (Florence), Italy.*

[c] *Department of Chemistry, University of Bari, 70126 Bari, Italy.*

[d] *LENS, European Laboratory for Non-linear Spectroscopy, Via N. Carrara 1, I-50019 Sesto F.no, (Florence), Italy.*

[e] *Institut de Chimie et procédés pour l'Energie, l'Environnement et la Santé (ICPEES), UMR 7515 CNRS-Université de Strasbourg, (Strasbourg), France.*

[f] *Shenyang National Laboratory for Materials Science, Institute of Metals Research, Chinese Academy of Sciences, 72 Wenhua Road, Shenyang, Liaoning, 110016, China*

[g] *Kazan Federal University, 420008 Kazan, Russian Federation.*

NMW	
C%	N%
89.02	3.24

r-NMW	
C%	N%
94.72	3.62

NMW@N$_1$$^{(Py)}$	
C%	N%
82,98	4,68

NMW@N$_2$$^{(Acr)}$	
C%	N%
85,39	4,76

MWCNT	
C%	N%
98,55	0,00

MWCNT@Acr^{OX}	
C%	N%
95,12	0,37

MWCNT@Acr^{OX} (blank test)	
C%	N%
93.98	0,00

Table S1. Elemental analyses for samples **NMW**, **r-NMW**, **NMW@N$_1$$^{(Py)}$**, **NMW@N$_2$$^{(Acr)}$**, pristine **MWCNTs**, **MWCNT@Acr^{OX}** (funct. Acridine N-oxide) and its blank functionalization test. The C% and N% contents are calculated as average values over three independent runs.

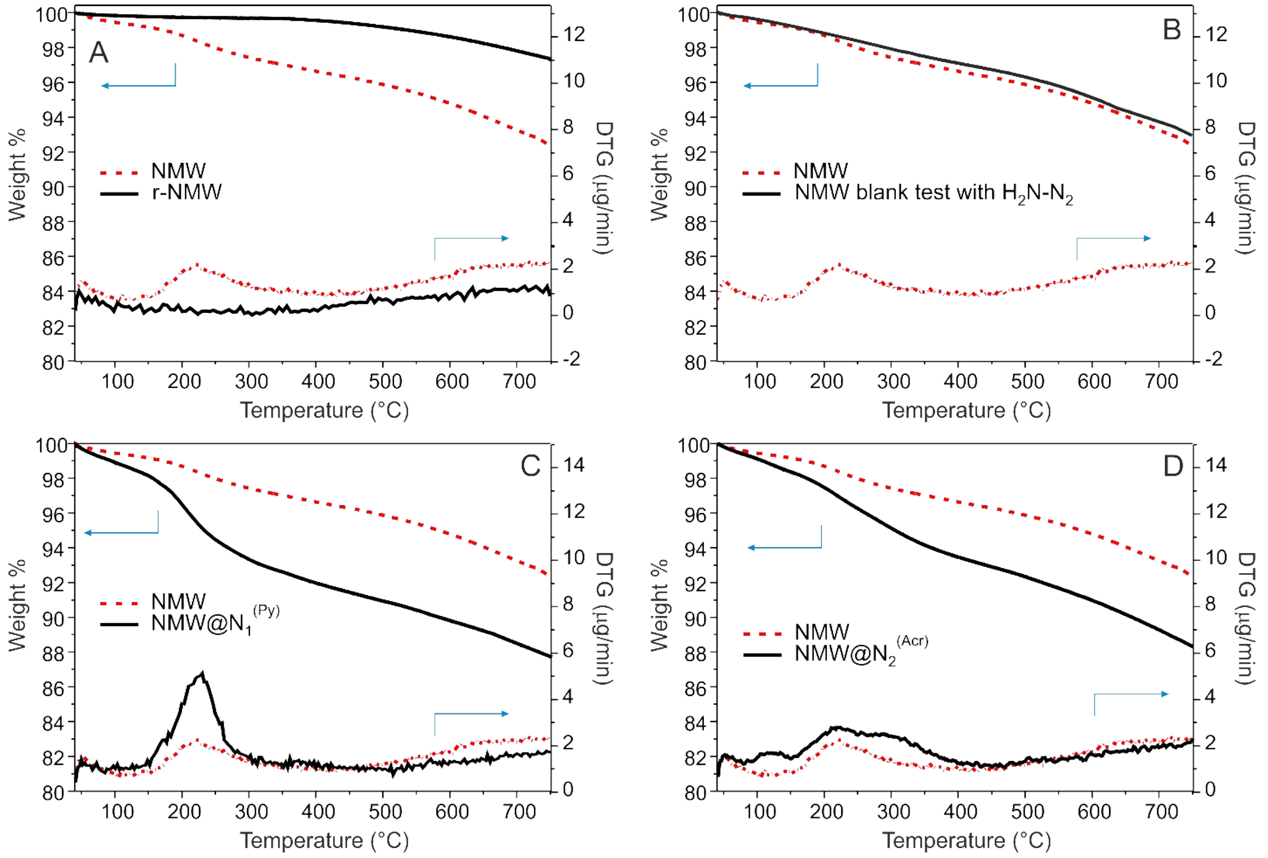

Fig. S1. TG/DTG profiles of **A**) NMW and r-NMW, B) NMW *vs*. blank test with H_2N-$N_2$$^{(Acr)}$, C) NMW *vs*. NMW@N$_1$$^{(Py)}$, D) NMW *vs*. NMW@N$_2$$^{(Acr)}$. Thermal programme: 40°C - 800 °C, 5°C/min; N_2 atm., 100 mL min^{-1}.

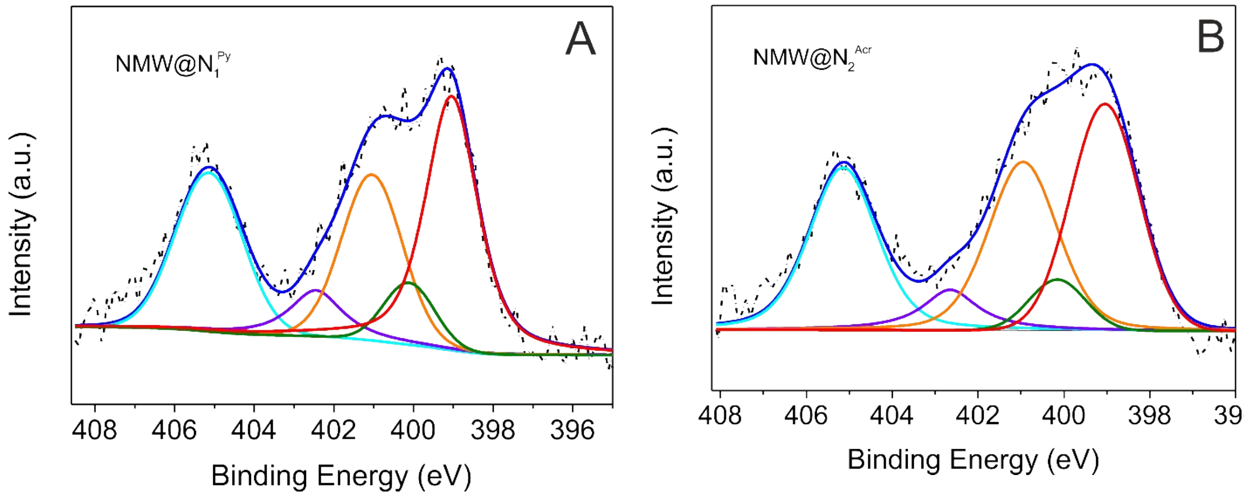

Fig. S2. High resolution N 1s core level regions of NMW@N$_1^{Py}$ and NMW@N$_2^{Acr}$ along with their related fits.

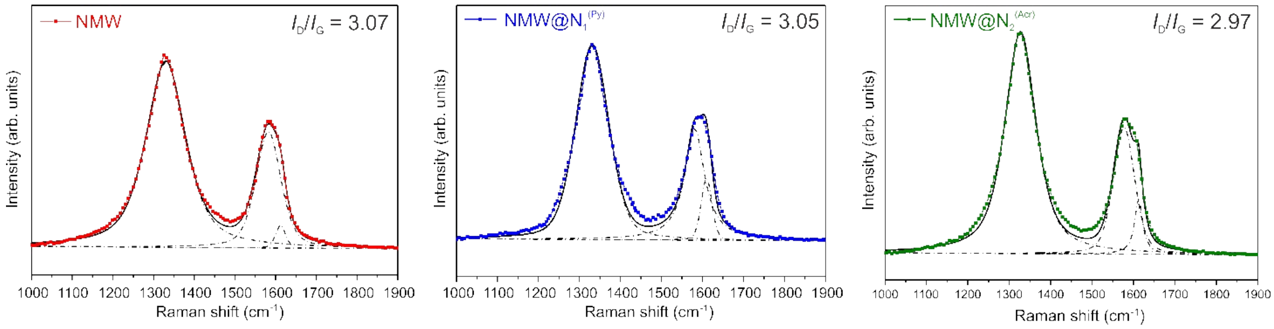

Fig. S3. Raman spectra of NMW and NMW@N$_{1-2}$ samples and their relative fits. Colored dots represent the experimental points. The single peak fittings are reported as dot-dashed lines (D, G and D' bands respectively in order of increasing relative wavenumbers), while the full line represents the total spectrum fit. All recorded curves were fitted using Voigt line shapes and the intensity ratios (namely, I_D/I_G) were calculated from the integrated intensity of the corresponding band.

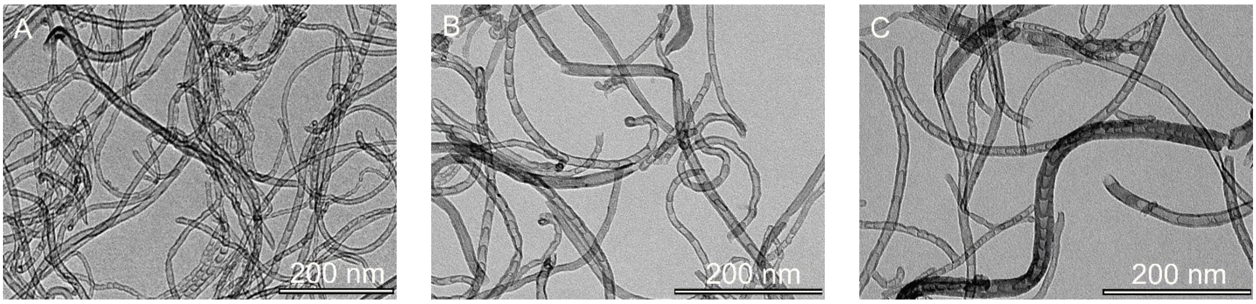

Fig. S4. TEM images of A) NMW and the N-functionalized derivatives B) NMW@N$_1^{(Py)}$ and C) NMW@N$_2^{(Acr)}$.

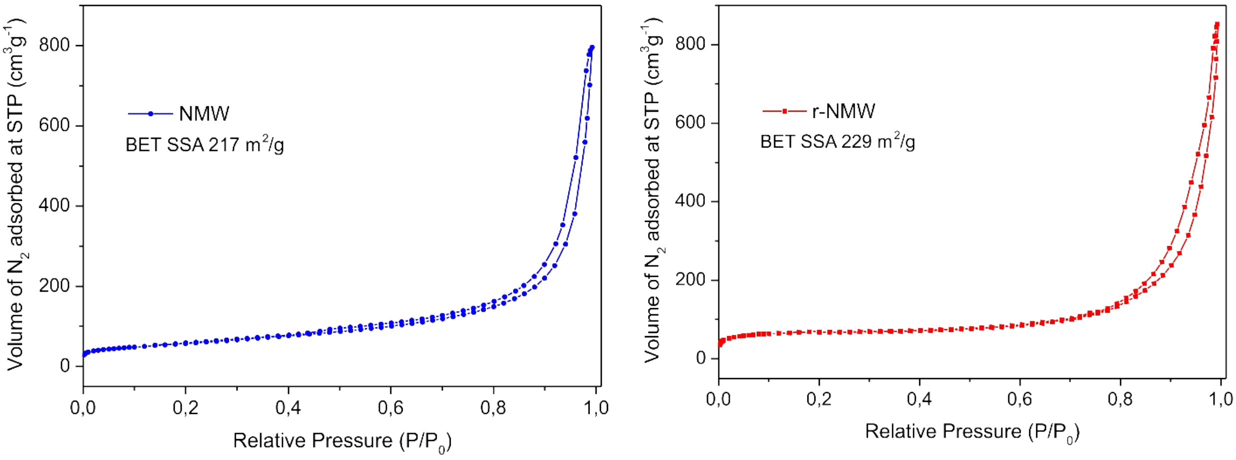

Fig. S5. Nitrogen adsorption-desorption isotherm linear plots (BET) of NMW (left) and r-NMW (right) recorded at 77 K.

Table S2. Acid-base titrations on the NMW, r-NMW and NMW@$\mathbf{N_{1\text{-}2}}$ samples.

	NMW		r-NMW
(1° run)	0.05	(1° run)	0.00
(2° run)	0.09	(2° run)	0.09
(3° run)	0.05	(3° run)	0.09
Calculated (N%) average value	0.06	Calculated (N%) average value	0.06

	NMW@$N_1^{(Py)}$		NMW@$N_2^{(Acr)}$
(1° run)	1.59	(1° run)	1.77
(2° run)	1.42	(2° run)	1.59
(3° run)	1.42	(3° run)	1.59
Calculated (N%) average value	1.48	Calculated (N%) average value	1.65

Table S3. Conductivity (σ) measurements on NMW and NMW@$N_2^{(Acr)}$ samples at 295 K.

Sample	t (m)	σ (S m^{-1})
NMW	$0.22*10^{-3}$	590
NMW@$N_2^{(Acr)}$	$0.24*10^{-3}$	615

Resistivity and conductivity were calculated according to the following equations.[1]

$$\rho = \frac{\pi}{\ln 2} \times t \times \frac{V}{I}; \qquad {}^{t}/_{s} \le 0.5;$$

ρ= resistivity (Ω m); t(film thickness - m); V (volt); I(Ampere); s = (inter probe spacing – m)

$$\sigma = \frac{1}{\rho}$$

σ= conductivity (S m^{-1}); ρ= resistivity (Ω m);

Synthesis of the 9-aminoacridine N-oxide. The synthesis of the 9-aminoacridine N-oxide reagent has been performed according to the synthetic path outlined in Scheme S1.

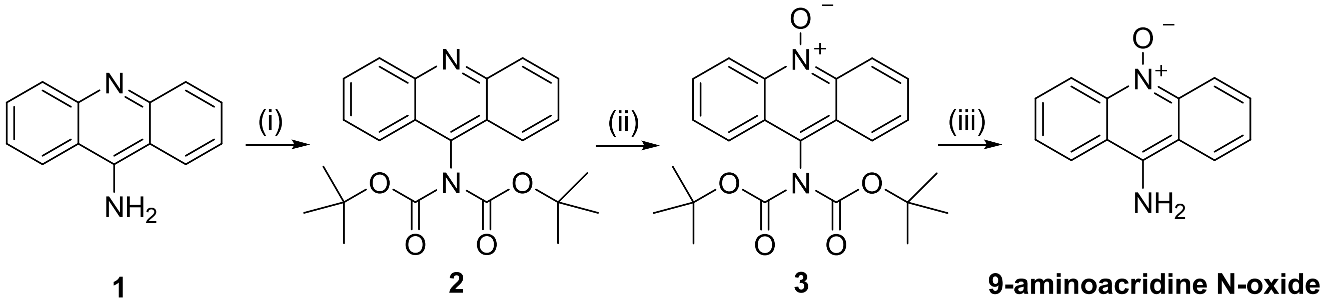

Scheme S1. Synthesis of the 9-aminoacridine N-oxide reagent. (i) Boc_2O, DMAP, CH_2Cl_2, reflux; (ii) mCPBA, CH_2Cl_2, r.t.; (iii) TFA:CH_2Cl_2, r.t.

Synthesis of the intermediate *9-di-tert-butyl acridin-9-ylcarbamate* (**2**). To a solution of 9-aminoacridine (**1**, 1.00 g, 5.15 mmol) in CH_2Cl_2 (22 mL) were added 4-dimethylaminopyridine (DMAP, 0.13 g, 1.03 mmol) and Boc anhydride (Boc_2O, 2.47 g, 11.33 mmol). The resulting mixture was refluxed overnight and then concentrated at reduced pressure. The crude solid residue was purified by chromatographic column on alumina (eluent: CH_2Cl_2/MeOH = 95/5) affording **2** as a pale yellow solid in 83 % yield. ^{1}H-NMR (400 MHz, CD_2Cl_2) δ (ppm): 1.21 (s, 18H), 7.62 (2H), 7.80 (2H), 8.02 (2H), 8.22 (2H). ^{13}C-NMR (100 MHz, CD_2Cl_2) δ (ppm): 27.7, 83.7, 123.0, 123.9, 127.2, 127.5, 130.3, 130.4, 141.5, 151.1. Elem. Anal. for $C_{23}H_{26}N_2O_4$: calc. (%): C 70.03, H 6.64, N 7.10; found: C 70.27, H 6.89, N 7.02.

Synthesis of the intermediate *9-((di-tert-butoxycarbonyl)amino)acridine 10-oxide* (**3**). To a solution of **2** (0.75 g, 1.90 mmol) in CH_2Cl_2 (100 mL) was added dropwise a solution of meta-chloroperbenzoic acid (mCPBA, 0.66 g, 3.8 mmol) in CH_2Cl_2 (50 mL). The resulting mixture was stirred at room temperature overnight. To the crude mixture was then added an aqueous solution of K_2CO_3 and the aqueous layer was extracted three times with CH_2Cl_2. The collected organic phases were dried over Na_2SO_4 and concentrated at reduced pressure. The crude material was purified by chromatographic column on alumina (eluent: petroleum ether/AcOEt = 80/20) to afford **3** as a yellow solid in 93 % yield. ^{1}H-NMR (400 MHz, CD_2Cl_2) δ (ppm): 1.23 (s, 18H), 7.67 (2H), 7.80 (2H), 8.00 (2H), 8.83 (2H). ^{13}C-NMR (100 MHz, CD_2Cl_2) δ (ppm): 27.8, 83.9, 120.4, 123.7, 125.6, 128.5, 128.8, 130.8, 140.4, 151.1. Elem. Anal. for $C_{23}H_{26}N_2O_5$: calc. (%): C 67.30, H 6.38, N 6.82; found: C 67.57, H 6.79, N 6.70.

Synthesis of 9-aminoacridine N-oxide. A solution of **3** (0.60 g, 1.46 mmol) in a 1 : 1 mixture of trifluoroacetic acid and CH_2Cl_2 (36 mL) was stirred at room temperature for 30 minutes. Afterwards the reaction mixture was concentrated at reduced pressure and the residual solid redissolved in MeOH. The solution was eluted through an ion exchange membrane (Amberlyst A-26(OH), Alfa Aesar) to afford **4** in pure form as a bright red solid in 95 % yield. ^{1}H-NMR (400 MHz, DMSO-d_6) δ (ppm): 7.46 (2H), 7.78 (2H), 7.90 (2H), 8.50 (2H), 8.62 (2H). ^{13}C-NMR (100 MHz, DMSO-d_6) δ (ppm): 112.8, 119.2, 123.5, 124.0, 131.3, 138.3, 142.3. Elem. Anal. for $C_{13}H_{10}N_2O$: calc. (%): C 74.27, H 4.79, N 13.33; found: C 74.18, H 4.92, N 13.29.

Electrochemical data processing.

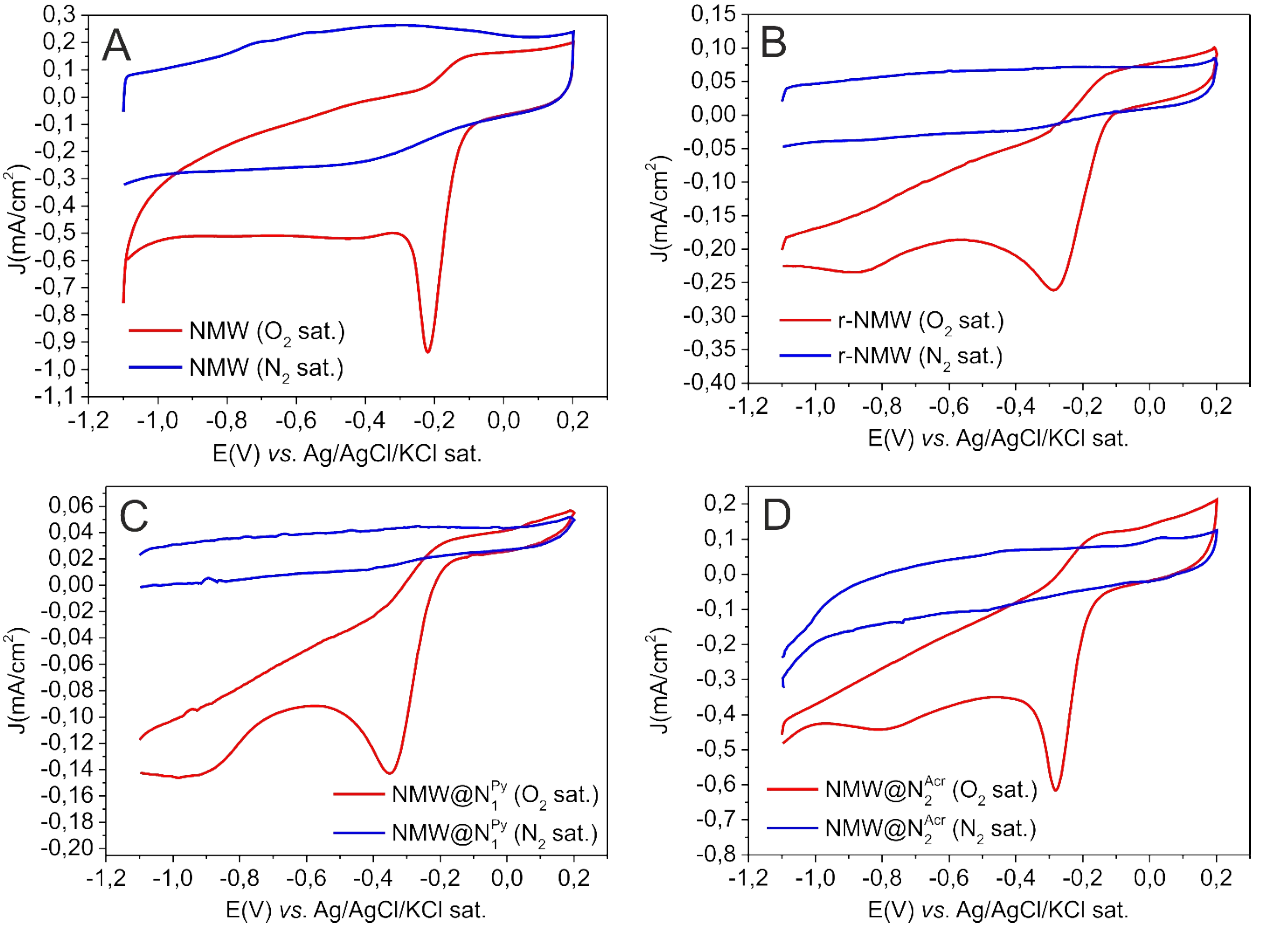

Fig. S6. Cyclic Voltammograms for the samples NMW (**A**), r-NMW (**B**), NMW@N$_1^{(Py)}$ (**C**) and NMW@N$_2^{(Acr)}$ (**D**) in N$_2$-saturated (blue-line) and O$_2$-saturated solutions (red-line). Scan rate of 5 mVs^{-1}. Ag/AgCl/KCl sat. was employed as reference electrode.

The amount of the N-containing nanomaterial deposited on the RRDE is maintained constant and fixed to the optimal value [catalyst loading (µg of NMW cm^{-2})] measured on the NMW sample.

Catalyst loading (mg of ink)	2.5	3	3.5
Catalyst loading (µg cm^{-2})	298	358	418
Catalyst loading (µg)[a]	58	70	82
Exchanged electrons (*n*)	3.68	3.92	3.76

[a] 0.196 cm^2 GC rotating-disk electrode

Table S4. Number of exchanged electrons for RRDE measurements carried out at different catalyst loadings (298, 358 and 418 µg cm^{-2}).

The ORR is studied through the RRDE measurements as described in the bodytext. The Pt Ring electrode potential is kept constant at a value of 0.5 V *vs*. Ag/AgCl/KCl sat. while the potential of the Disk electrode is swept from -1.1 V to 0.2 V and reversed against an Ag/AgCl/KCl sat. as reference electrode with a scan rate of 5 mVs^{-1}. The Ring potential value is chosen to allow only the oxidation of H_2O_2 [2]. While the total Disk current I_D is the sum of the O_2 reduction current to H_2O (I_{H2O}) and to H_2O_2 (I_{H2O2}) (eq.1), the Ring current I_R is due to the H_2O_2 oxidation (I_{H2O2}) exclusively (eq.2).

$$I_D = I_{H_2O} + I_{H_2O_2} \quad \text{(eq. 1)}$$

$$I_R = I_{H_2O_2}N \quad \text{(eq. 2)}$$

N is the Collection Efficiency [3] and it is the fraction of the material from the disk which subsequently flows at the ring electrode. It can be expressed as a fraction between 0.0 and 1.0 and depends on the electrode geometry. In this work we make use of the theoretical Collection Efficiency of 0.256 as reported for the employed Pine RRDE electrode.

Accordingly, the molar fraction of H_2O_2 (X_{H2O2}) produced in the process is calculated from the number of moles of H_2O (n_{H2O}) and H_2O_2 (n_{H2O2}) using the following equations:

$$n_{H_2O} = \frac{I_{H_2O}}{4F} \quad (eq.3)$$

$$n_{H_2O_2} = \frac{I_{H_2O_2}}{2F} \quad (eq.4)$$

$$X_{H_2O_2} = \frac{n_{H_2O_2}}{n_{H_2O_2} + n_{H_2O}} \quad (eq.5)$$

Replacing moles with the experimental currents (I_D and I_R) as calculated from eqs. 1 and 2 we obtain eq. 6:

$$X_{H_2O_2} = \frac{2I_R/N}{I_D + I_R/N} \quad (eq.6)$$

The number of electrons transferred per O_2 molecule in the ORR for the different catalysts has been calculated by the Koutecky-Levich equation applied to the ORR curves obtained at different rotation rates (rpm) [4]. The Koutecky-Levich equation is given by eq 7:

$$\frac{1}{j} = \frac{1}{j_{cc}} + \frac{1}{nK_f\sqrt{f}} \qquad \text{(eq. 7)}$$

With:

$$K_f = 0{,}2FC_0D_0^{2/3}\nu^{-1/6}$$

Where, j is the current density, j_{cc} is the kinetic current density, n is the number of exchanged electrons, F is the Faraday constant, D_0 is the oxygen diffusion coefficient (1.95 x 10^{-5} cm^2 s^{-1}), f is the angular rotation rate of the electrode (rpm), ν is the kinematic viscosity of the solution (0.008977 cm^2 s^{-1}) and C_0 is the O_2 concentration in solution (1.15 x 10^{-3} mol dm^{-3}). With these parameters, the value of K_f constant is 0,03538. The average number of electrons n exchanged during the ORR has been extrapolated from the slop of the plot of j^{-1} versus $f^{-1/2}$ at a specific potential value. We have recorded cyclic voltammetries from -1.1 V to 0.2 V at different rotation rates (from 400 to 2000 rpm) and calculated the n values at -0.95, -0.85, -0.75 and -0.65 V.

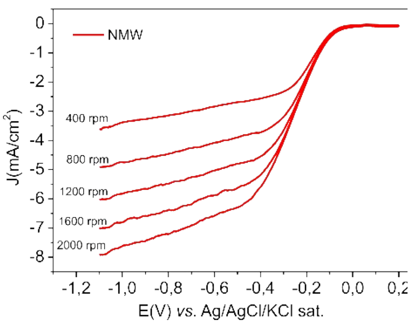

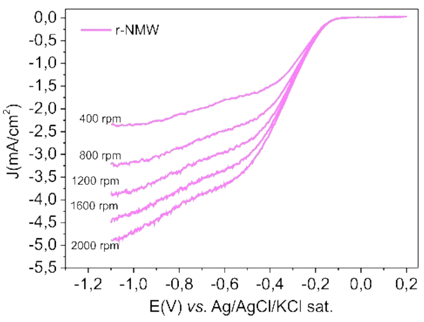

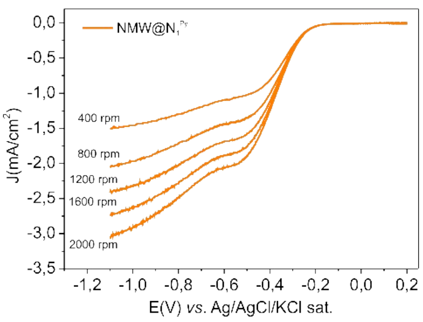

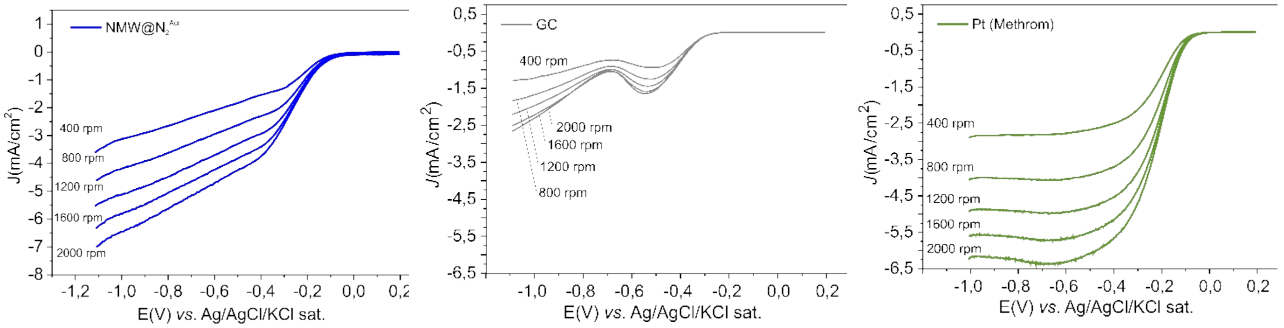

Fig. S7. Linear sweep voltammograms (LSVs) for ORR in O_2-saturated 0.1 M KOH solution for NMW, r-NMW, NMW@N_{1-2} samples, GC and the Pt-based reference electrode, at variable spin rates (400, 800, 1200, 1600 and 2000 rpm). Scan rate: 5 mV s^{-1}, catalyst loading 358 μg cm^{-2}.

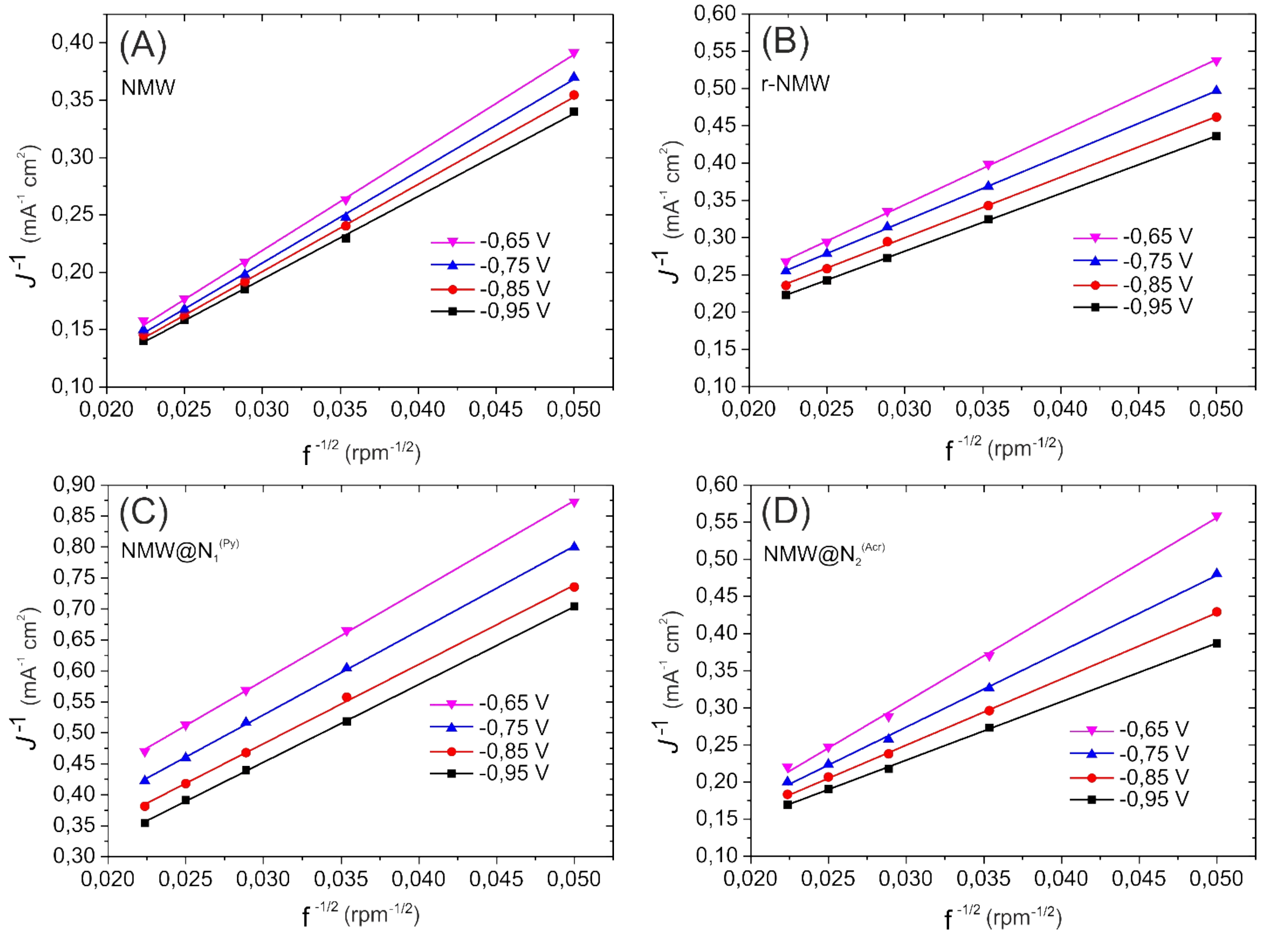

Fig. S8. *K-L* plots for NMW (**A**), r-NMW (**B**), NMW@$N_1^{(Py)}$ (**C**), NMW@$N_2^{(Acr)}$ (**D**) as obtained from the respective LSVs at -0.65 (pink line), -0.75 (blue line), -0.85 (red line) and -0.95 V (black line), respectively. Parameters used: O_2 concentration (C), 1.15 10^{-3} mol L^{-1}; O_2 diffusion coefficient (D), 1.95 10^{-5} cm^2 s^{-1}; kinematic viscosity (ν) of the electrolyte solution, 0.008977 cm^2 s^{-1}.

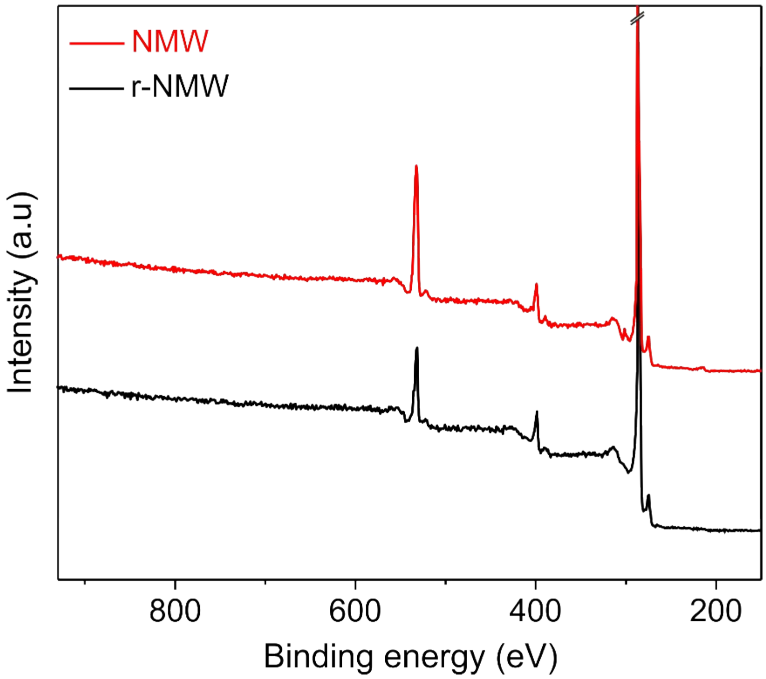

Fig. S9. XPS survey spectra NMW (red line) and its reduced counterpart (r-NMW – black line). Iron-based contaminants should appear in the XPS Fe 2p core region between 705-735 eV (Fe $2p_{1/2}$, Fe $2p_{3/2}$). Both XPS survey spectra and high resolution Fe 2p core level region do not show any contribution from this element.

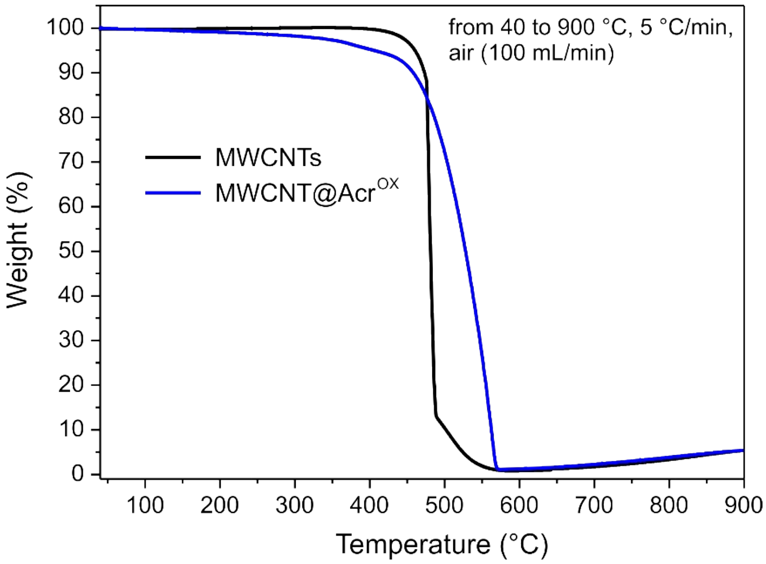

Fig. S10. TG/DTG profiles of pristine MWCNT (black line) and MWCNT@Acr^{OX} (blue line) samples.

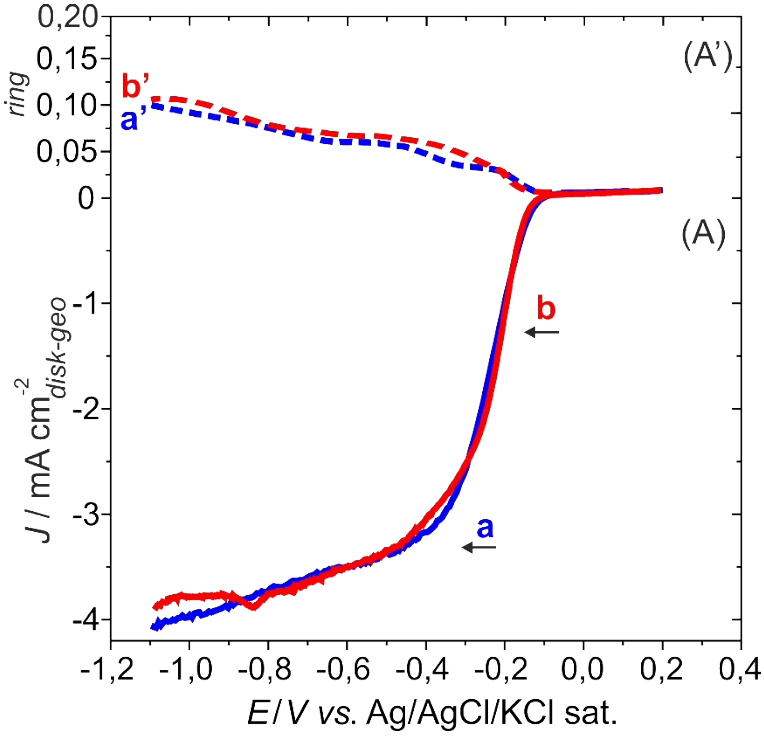

Fig. S11. (A) RRDE current–potential curves of MWCNT@Acr (curve a and a' – blue lines) and MWCNT@Acr^{OX} (curves b and b' – red lines) at the regime conditions (≥ 20 cycles) at 293 K for ORR in O_2 saturated 0.1 M KOH solution recorded by using a rotating ring-disk GC electrode [GC disk, A = 0.196 cm^2] with (A') Pt ring [A = 0.11 cm^2] held at a potential of 0.50 V. All samples are measured at an angular rotation rate (f) of 800 rpm with a scan rate of 5 mV s^{-1}. RRDE of MWCNT@Acr have been reported elsewhere (see ref. [5]) and outlined here for the sake of completeness.

References

1. L. I. Maissel and R. Glang *Hand book of Thin Film technology*, MC Graw Hill Co., New York, USA, 1970.
2. Y. Wang, D. Zhang and H. Liu, *J. Power Sources*, 2010, **195**, 3135-3139.
3. W. J. Albery and S. Bruckenstein, *Trans. Faraday Soc.*, 1966, **62**, 1920-1931.
4. S. Treimer, A. Tang and D. C. Johnson, *Electroanalysis*, 2002, **14**, 165-171.
5. G. Tuci, C. Zafferoni, P. D'Ambrosio, S. Caporali, M. Ceppatelli, A. Rossin, T. Tsoufis, M. Innocenti and G. Giambastiani, *ACS Catal.*, 2013, **3**, 2108-2111.